Effect of the Exchange-Correlation Potential on the Transferability of Brønsted-Evans-Polanyi Relationships in Heterogeneous Catalysis

José L. C. Fajín,[≠] Francesc Viñes,[‡] M. Natália D. S. Cordeiro,[≠] Francesc Illas,[‡] and José R. B. Gomes[§*]

[≠]*LAQV@REQUIMTE, Faculdade de Ciências, Universidade do Porto, P-4169-007 Porto, Portugal.*

[‡]*Departament de Química Física & Institut de Química Teòrica i Computacional (IQTCUB), Universitat de Barcelona, c/Martí i Franquès 1, 08028 Barcelona, Spain.*

[§]*CICECO – Aveiro Institute of Materials, Departamento de Química, Universidade de Aveiro, 3810-193 Aveiro, Portugal.*

*Corresponding author, e-mail: jrgomes@ua.pt ; Fax: +351 234401470

Abstract

As more and more accurate density functional methods emerge, the transferability of Brønsted-Evans-Polanyi (BEP) relationships obtained with previous models is an open question. In this work, BEP relationships derived from different density functional theory based calculations are analyzed to answer this question. In particular, BEP relationships linking the activation energy of O–H bond breaking reactions taking place on metallic surfaces with the adsorption energy of the reaction products are chosen as case study. These relationships are obtained with the widely used Perdew-Wang (PW91) Generalized Gradient Approximation (GGA) exchange-correlation functional and with the more accurate meta-GGA Tao-Perdew-Staroverov-Scuseria (TPSS) one. We provide compelling evidence that BEP relationships derived from PW91 and TPSS functionals are essentially coincidental. This finding validates previously published BEP relationships and indicates that reaction activation energy barrier can be obtained by the determination of the energy reaction descriptor value at the less computationally demanding GGA level; an important aspect to consider in future studies aimed at the computational design of catalysts with improved characteristics.

Keywords

Heterogeneous Catalysis; Density Functional Theory; Adsorption; Reaction Descriptors; BEP Relationships

Research in heterogeneous catalysis is being greatly assisted by computational methods aimed at a rational design of catalysts with improved characteristics for a specific reaction.[1-3] Valuable information that is not easily experimentally obtained can be retrieved from computational results such as the determination of most keen catalyst reactive sites, the unfolding of reaction mechanisms, and the overall reaction energetics. When combined with experimental evidences, the computational data may be also used to understand the effects of the catalyst structure and composition in its reactivity.[2-3,5] Among the different classes of theoretical methods that have been used so far in heterogeneous catalysis, those based on Density Functional Theory (DFT) are the most used because of their good ratio between results quality and computational expenditures.1 Such approaches have been shown to provide a very good description of the thermodynamics and kinetics of a particular reaction occurring on a specific catalyst.[6]

When compared with the determination of the thermodynamic energy profile for a specific reaction, obtaining kinetic data is computationally expensive and challenging since it involves the location of the Transition State (TS) structure corresponding to each elementary reaction step. This process needs to be repeated for all elementary steps involved in the full reaction path. The difficulties associated with the determination and characterization of TS structures can be circumvented with the usage of Brønsted-Evans-Polanyi (BEP) relationships,[1,7,8] linearly relating the activation energy of a reaction, *i.e.*, the quantity difficult to obtain, with a descriptor more easily calculated, in this case, either the reaction energy (classical BEP) or the adsorption energy of a species involved in the reaction. Some relevant examples reported in the literature of BEP relationships based on extensive sets of DFT calculations concerning the adsorption and reaction of molecules on metal surfaces are those due to

Pallassana and Neurock for ethylene (de)hydrogenation,[9] to Nørskov *et al.* for the dissociation reactions of N_2, O_2, CO, and NO diatomic molecules,[10] and Loffreda *et al.* for the hydrogenation of unsaturated aldehydes.[11] These BEP relationships have spread beyond metal substrates going for oxide and carbide compounds.[12,13]

From the computational point of view, and when comparing to the energy of reaction, the adsorption energy of a specific species is a more interesting descriptor simply because the calculation of the reaction energy nurtures from knowing the reaction path which, in turn, requires determining the structures and energies of both adsorbed reaction reagents and products. Thus, BEP relationships anchored on quantities easily calculated, *e.g.*, the adsorption energy of a species involved in the reaction, are more interesting for practical screening purposes. We have been previously deeply involved in the determination of BEP relationships based on these descriptors, especially for the exemplary O-H bond dissociation in water, methanol, and ethanol on metal based surfaces and nanoparticles,[4,5,14-16] and found that the adsorption energy of a simple species, *e.g.* an oxygen adatom, can be an interesting descriptor.[14] Unfortunately, for a BEP with more universal characteristics for a specific reaction,[17] the latter descriptor is not useful because the activation energy predicted by the relationship would be the same for any molecule on the same catalyst surface model.[17] Thus, for reaching such a generic behavior, the descriptor must be related with the structural specificities of the molecules that are reacting on the catalyst surface. Based on energetic data obtained with the Perdew-Wang (PW91)[18] exchange-correlation functional, within the Generalized Gradient Approximation (GGA), Fajín *et al.* found that the adsorption energy of the reaction products was an adequate descriptor for the O-H bond dissociation reactions of different molecules on several different metal based catalyst models.[17] The same authors found that the activation energy barrier for H_2O dissociation on Cu(111)

calculated with the PW91 and the Perdew-Burke-Ernzerhof (PBE)[19] functional are very similar with values of ~0.92 and 0.93 eV,[20] respectively. This values are in satisfactory agreement with the experimental value (0.74 eV),[21] based on the apparent activation energy for the water gas shift reaction on the Cu(111) surface. In a similar way, Mohsenzadeh *et al.*[22] estimated the activation energy barriers for the water molecule dissociation on Ni(100), Ni(110), and Ni(111) using the adsorption energy calculated with PBE for co-adsorbed OH and H on the corresponding Ni surfaces, and the BEP equation reported by Fajín *et al.*[17] derived from PW91 and found that the estimated values differed by less than 0.06 eV. Nevertheless, both PW91[18] and PBE[19] stem from the GGA approach, both methods are functionals from the second rung of Jacob's ladder of DFT approximations to the exchange-correlation energy[23] and, hence, these findings are not unexpected. As more and more accurate exchange-correlation functionals of different types are emerging aimed at improving the description of energy related properties in molecular systems[24] one may wonder whether the information extracted from less accurate DFT methods remains valid. In other words, are PW91 BEP relationships transferable? Is PW91 able to cope with descriptors calculated with other levels of theory? This question is pertinent since GGA type functionals are known to perform very well for metallic systems[25] but are known to have problems in accurately describing the thermochemistry of molecular systems.[26]

Among the different density functionals beyond GGA, those belonging to the meta-GGA and to the Non-separable Gradient Approximation (NGA) have been suggested to be promising for the description of metallic systems. In fact, recent studies focused in the calculation of bulk properties of the three series of transition metal systems with different DFT functionals[27] showed that the Tao−Perdew−Staroverov−Scuseria (TPSS)[28] and the local Minnesota 06 (M06-L)[29] meta-GGA functionals, and the local Minnesota 12 (MN12-L)[30] meta-NGA functional, have an

accuracy similar to that demonstrated by PBE for bulk properties of transition metal systems.[31] Since the meta-GGA functionals are found to provide better molecular properties than the GGA ones for systems containing main group elements,[32-35] approaches such as TPSS and M06-L appear to be very convenient for properly describing the interaction of molecules with solid-state systems containing transition metals. In fact, recent studies suggest that M06-L is an interesting approach for such kind of calculations,[36-38] plus both TPSS and M06-L functionals do rather accurately describe core level binding energy of main group elements.[39,40] In clear contrast, hybrid density functionals, broadly used to describe molecular systems,[26] are not suitable to describe the chemistry of molecules at metallic surfaces because *i)* when combined with plane wave basis sets, they originate a singularity that slows down the convergence with the density of k-points in the reciprocal space,[41] and *ii)* provide a poor description of bulk metals.[27]

From the discussion above we can surmise that the TPSS functional is a good compromise when aiming at simultaneously describing molecules and metallic surfaces. To further proof this hypothesis here we study the validity of previously derived BEP relationships[17] by computing at the TPSS level the adsorption and co-adsorption energy as well as activation energy barriers for O-H bond cleavage of a series of molecules above a broad number of metallic surfaces. Water (HO-H), methanol (CH_3O-H), and ethanol (CH_3CH_2O-H) molecules are selected as examples of RO-H compounds. The O-H dissociation on these compounds is studied on metal surface catalyst models that showed high, moderate, and low activity towards the breakage of the O-H bond, as shown in Ref. 17. More precisely, Cu(110), Cu(111), Ir(111), Pd(111), Rh(211), and Au(111) surface slabs were used for water, Cu(110), Ir(111), Pd(111), Rh(211), Ni(111), Ag(110), and Pt(111) for methanol, and the Cu(111) surface was used for ethanol. To this end TPSS calculations have been carried out for the determination and characterization of the initial

(molecular ROH adsorption), final (adsorption of the separated $RO^{\cdot}$ and $H^{\cdot}$ fragments), and transition (energy of the transition state structure associated with the cleavage of the RO-H bond) states for the generic reaction:

$$\text{RO-H (ads)} \rightarrow \text{RO}^{\cdot}\text{ (ads)} + \text{H}^{\cdot}\text{ (ads)} \qquad (1)$$

at the considered (110), (111), and (211) surfaces of several transition metals. Possible adsorption sites are shown in Figure 1 and selected structural and energetic parameters for each of the three states are reported in Tables 1, 2, and 3, respectively.

As can be seen in Table 1, the preferred adsorption sites predicted by TPSS and PW91 are the same and nearest-neighbor distances calculated for the molecular adsorbates are very much close, with deviations of 0.05 Å in average. The largest difference is found for methanol adsorption on Pt(111) with a difference of 0.12 Å. These differences are also reflected in the values of the adsorption energy (E^{o}_{ads}), calculated as:

$$E^{o}_{ads} = E^{o}_{slab-ROH} - E^{o}_{slab} - E^{o}_{ROH} \qquad (2)$$

where $E^{o}_{slab-ROH}$, E^{o}_{slab}, and E^{o}_{ROH} denote the total energies incorporating Zero Point Vibrational Energy (ZPVE) corrections of the adsorbate-slab system (molecular and dissociated for initial and final states, respectively), of the bare metal slab, and of the adsorbate isolated in the gas-phase, respectively. The separate analysis of the adsorption energies calculated for the three molecular adsorbates shows that TPSS values are systematically less negative (0.15 eV in average) than those calculated with PW91 in the case of water, very similar in the case of methanol (maximum difference of 0.04 eV), and more negative in the case of ethanol (0.14 eV). The interaction energies for the products of the reactions of water, methanol, and ethanol O-H

bond dissociations on the different metal surfaces are reported in Table 2. Again, with a few exceptions only, the co-adsorption energies, adsorption sites, and oxygen to surface distances calculated with the TPSS and PW91 functionals are very similar. Still, in general, the co-adsorption energies calculated with the meta-GGA approach are systematically lower (more favorable adsorption) than those computed with PW91, of 0.10 eV in average, being the co-adsorption energy of the products of the water dissociation on Rh(211) the exception. The most significant energy (0.2 eV) difference is found for the interaction of the methanol dissociation products, e.g. co-adsorbed methoxy and hydrogen species, on the Pd(111) surface.

The calculated activation energy barriers and the reaction energies for the O-H bond cleavages in water, methanol, and ethanol on the considered surface models are given in Table 3, together with selected parameters for the transition states connecting the initial and final state configurations found on each surface. The activation energy barriers ($E_{\mathrm{act}}^{\mathrm{o}}$) were calculated as the difference between the TS energy and that of the initial state, the latter corresponding to the most stable configuration for adsorbed reactants. From Table 3 it appears that the TPSS calculated activation energy barriers are lower than those obtained with PW91, with a single exception; the dissociation of the O-H bond in ethanol on the Cu(111) surface, but where it is larger by only 0.02 eV. The decrease in the activation energy barriers on going from GGA to meta-GGA are more noticeable in the cases of water dissociation on Pd(111) and Au(111), by 0.1 eV. In the remaining cases, i.e., water dissociation on Ir(111) and methanol O-H bond breaking on the seven surfaces considered, the differences between TPSS and PW91 energy barriers are more modest (cf. < 0.1 eV). In the TS structures, the length of the O-H suffering cleavage is slightly more elongated when the dimer approach is used with the PW91 method than when combined with the TPSS functional. Finally, the reaction energies calculated with the TPSS density

functional are more negative than those obtained with PW91 by ~0.2 eV. This behavior is expected because, as found previously,[4,5,14-17] reactions thermodynamically more favorable have associated smaller activation energy barriers. Aside, the stronger attachment of dissociated states at TPSS level implies de facto a reaction energy barrier lowering. Here it is worth to stress out that the stronger attachment by TPSS compared to PW91, and so, the reaction energy barrier lowering, implies that the transition state theory (TST) derived rates predicted by TPSS are generally larger than the ones obtained by PW91. In average terms, this implies that the TST rates from TPSS calculations are in between half and one order of magnitude larger than the ones obtained by PW91, and so, this has to be kept in mind when dealing with kinetic aspects. However, such a feature does not affect the BEP relationships, as shown below.

Plotting the activation energy barriers against the adsorption energies of the products evidences a noticeable correlation as clearly seen in Figure 2 and already commented in previous work. However, Figure 2 introduces a very important feature. For the two different sets of adsorption and activation energies obtained from TPSS and PW91 calculations, the separate regression analyses point to a very similar dependence of the two quantities. Consequently, one can surmise that the emerging relationship is not only general for reactions at metallic surfaces involving the dissociation of the O-H bond of adsorbed molecules,[17] but that it is also independent of the computational approach, thus having an universal character. In other words, climbing rungs on the DFT Jacob's ladder does not invalidate conclusion from BEP relationship established from less accurate functionals. This is a very relevant conclusion since it validates previous studies while paving the road for a practical computational screening of metal-based surfaces for catalytic applications at more affordable computational levels and for a rational design of catalysts with improved characteristics.

Computational Methods

All the DFT calculations were performed with the VASP 5.3 computer code[42-44] using the TPSS meta-GGA density functional.[28] The comparison is made with results from previous calculations employing the PW91 functional.[17] The valence states were described by a plane wave basis set with a cutoff of 415 eV for the kinetic energy while the effect in the valence electronic density of the core electrons was taken into account using the projected augmented-wave (PAW) method as implemented in VASP.[45,46] The numerical integration in the reciprocal space was done considering a 7×7×1 Monkhorst-Pack grid of special **k**-points[47] and the ions were relaxed using a conjugate-gradient algorithm.

The dimer approach[48] was considered in the search of transition states (TS) structures applying very strict convergence criteria (10^{-6} eV for the total energy change and 10^{-3} eV/Å for the forces acting on the ions), which is necessary to avoid the algorithm stopping at local minima, being this especially important in the case of calculations involving stepped surface models —*e.g.* (211) Miller index models—. The TS structures obtained were confirmed by a vibrational frequency analysis where it is obtained a single imaginary frequency in the normal mode driving toward products.

The metallic surfaces, namely, Ag(110), Au(111), Cu(110), Cu(111), Ir(111), Ni(111), Pd(111), Pt(111), and Rh(211) are represented in this work by periodic slab models with the repeated slabs separated, as usual, with a vacuum region of ~10 Å, which is large enough to avoid interactions with neighboring replicas. The slab models for the (111) and (110) Miller index surfaces are 2×2 representations of the unit supercell, while a 2×1 representation is considered for the (211) Miller index surface. The slab models have a thickness corresponding to four

atomic layers. The lattice vectors for each bulk metal were optimized using the same computational approach as common practice.

By applying also the same computational setup, the most stable adsorption geometries for water, methanol, or ethanol as well as for the corresponding dissociation products were obtained by full relaxation of the adsorbate(s) atomic positions and of two top metallic layers, while the two bottom metallic layers were kept frozen to simulate the bulk metal, *i.e.* 2+2 approach.

Adsorption and activation energies were ZPVE corrected according with the harmonic oscillator approach and considering the vibrational frequencies calculated. We also made an estimation of the rates (k) for the reactions studied using the equation below derived from transition state theory (TST),[49]

$$k = \left(\frac{k_B T}{h}\right)\left(\frac{q^{\neq}}{q}\right) e^{\frac{-E^{o}_{act}}{k_B T}} \qquad (3)$$

where $q^{\neq}$ and q are the vibrational partition functions for the TS and IS, respectively, which have been approximated from the harmonic vibrational frequencies, k_B is the Boltzmann constant, T is the absolute temperature, h is the Planck constant, and E^{o}_{act} is the zero point corrected activation energy barrier. A temperature of T = 463 K, typical for the water gas shift reaction,[50] was considered in the calculation of the TST rates of different reactions on surfaces.

Acknowledgments

This work was developed within the scope of the projects CICECO-Aveiro Institute of Materials, POCI-01-0145-FEDER-007679 (FCT Ref. UID/CTM/50011/2013), LAQV@REQUIMTE (UID/QUI/50006/2013), and CODECAT (PTDC/QUI-QUI/117439/2010-FEDER-020977), financed by national funds through the FCT/MEC and when appropriate co-financed by FEDER under the PT2020 Partnership Agreement. J.L.C.F. and J.R.B.G. acknowledge FCT for the grant SFRH/BPD/64566/2009 cofinanced by the Programa Operacional Potencial Humano (POPH) / Fundo Social Europeu (FSE) and Quadro de Referência Estratégico Nacional 2009-2013 do Governo da República Portuguesa, and for the Programme Investigador FCT, respectively. The research carried out at the *Universitat de Barcelona* was supported by the Spanish MINECO grant CTQ2015-64618-R grant and, in part, by *Generalitat de Catalunya* (grants 2014SGR97 and XRQTC). F.V. thanks the MINECO for a postdoctoral *Ramón y Cajal* (RyC) research contract (RYC-2012-10129).

Table 1. TPSS Calculated Adsorption Energies (E^{o}_{ads}, eV) and Distances (Å) for H_2O, CH_3OH, and CH_3CH_2OH on Several Metallic Surfaces. For Comparison PW91 Values Are Given in Parenthesis.

Surface	Species	E^{o}_{ads}	Adsorption site[a]	d[b]
Cu(110)	H_2O	-0.28 (-0.42)	T	2.18 (2.19)
Ir(111)		-0.19 (-0.32)	T	2.34 (2.38)
Pd(111)		-0.14 (-0.30)	T	2.43 (2.45)
Rh(211)		-0.41 (-0.55)	B_S	2.29 (2.29)
Au(111)		-0.01 (-0.18)	T	2.98 (2.90)
Cu(111)		-0.06 (-0.22)	B	2.42 (2.50)
Cu(110)	CH_3OH	-0.24 (-0.24)	B	2.32 (2.33)
Ni(111)		-0.04 (-0.04)	physisorbed	2.74 (2.67)
Pd(111)		-0.01 (-0.03)	physisorbed	2.69 (2.58)
Rh(211)		-0.36 (-0.35)	B_S	2.38 (2.42)
Ag(110)		-0.12 (-0.15)	B	2.71 (2.73)
Ir(111)		-0.02 (-0.04)	physisorbed	2.90 (2.85)
Pt(111)		0.00 (-0.04)	physisorbed	2.95 (2.83)
Cu(111)	CH_3CH_2OH	-0.32 (-0.18)	T	2.51 (2.48)

[a]Notation for adsorption sites (ROH species) is provided in Figure 1. Physisorbed state is used to denote methanol adsorption orientations with the hydroxyl hydrogen pointing to the surface.

[b]Nearest-neighbor distance between atoms from the adsorbate and from the surface.

Table 2. TPSS Calculated Co-adsorption Energies (E^{o}_{coads}, eV) and Adsorbate to Surface Distances of the Co-adsorbed OH+H, CH_3O+H, and CH_3CH_2O+H Species on Several Metallic Surfaces. For Comparison PW91 Values Are Given in Parenthesis.

Surface	**Species**	E^{o}_{coads}	**Adsorption site**[a]	**d**[b]
Cu(110)	OH+H	-0.42 (-0.38)	B / C_3	1.97 (1.97)
Ir(111)		0.07 (0.11)	B / F	2.18 (2.18)
Pd(111)		0.07 (0.11)	F / H	2.16 (2.17)
Rh(211)		-0.89 (-0.96)	B_S / B_S	2.10 (2.10)
Au(111)		1.50 (1.59)	B / F	2.25 (2.27)
Cu(111)		-0.10 (-0.07)	F / F	2.01 (1.69)
Cu(110)	CH_3O+H	-0.49 (-0.44)	B / B	1.96 (1.95)
Ni(111)		-0.73 (-0.53)	F / F	1.99 (1.98)
Pd(111)		-0.04 (0.17)	F / F	2.15 (2.13)
Rh(211)		-1.12 (-0.96)	B_S / B_S	2.07 (2.08)
Ag(110)		0.39 (0.49)	B / B	2.21 (2.22)
Ir(111)		0.11 (0.25)	B / T	2.17 (2.18)
Pt(111)		0.41 (0.54)	B / B	2.15 (2.16)
Cu(111)	CH_3CH_2O+H	-0.12 (-0.03)	F / H	2.05 (2.04)

[a]Notation for adsorption sites (RO / H species) is provided in Figure 1.

[b]Nearest-neighbor distance between the oxygen and surface metal atoms, in Å.

Table 3. TPSS Calculated Activation Energy Barriers (E^{o}_{act}, eV), Reaction Energies (E^{o}_{react}, eV), and TST Rates (k, s^{-1}) for the Reactions of O-H Bond Dissociation of Water, Methanol, and Ethanol on Several Metallic Surfaces. The Imaginary Frequency (υ, cm^{-1}), and the Length of the O-H bond ($d_{O\cdots H}$, Å) in the Transition State Are Also Compared. For Comparison PW91 Values Are Given in Parenthesis.

Surface	**Species**	E^{o}_{act}	E^{o}_{react}	***k* (463 K)**	**υ**	$d_{O\cdots H}$
Cu(110)	H_2O	0.52 (0.61)	-0.14 (0.03)	4.5×10^{6} (4.0×10^{5})	1374 (1262)	1.40 (1.43)
Ir(111)		0.65 (0.68)	0.26 (0.43)	3.4×10^{5} (1.7×10^{5})	836 (714)	1.50 (1.54)
Pd(111)		0.86 (0.96)	0.21 (0.41)	6.9×10^{2} (5.1×10^{1})	616 (532)	1.64 (1.70)
Rh(211)		0.66 (0.67)	-0.46 (-0.41)	2.6×10^{5} (1.2×10^{5})	1129 (1086)	1.45 (1.47)
Au(111)		1.78 (1.88)	1.51 (1.64)	6.4×10^{-9} (1.5×10^{-9})	381 (347)	1.98 (2.01)
Cu(111)		0.88 (0.91)	-0.04 (0.15)	3.0×10^{2} (1.6×10^{2})	1325 (1228)	1.43 (1.47)
Cu(110)	CH_3OH	0.42 (0.48)	-0.25 (-0.19)	1.2×10^{7} (6.3×10^{6})	1310 (1215)	1.42 (1.46)
Ni(111)		0.44 (0.48)	-0.68 (-0.48)	3.9×10^{7} (1.5×10^{7})	831 (770)	1.51 (1.53)
Pd(111)		0.68 (0.73)	-0.03 (0.18)	1.1×10^{5} (6.4×10^{4})	692 (640)	1.60 (1.64)
Rh(211)		0.27 (0.31)	-0.77 (-0.61)	1.1×10^{10} (2.8×10^{9})	1338 (1237)	1.38 (1.41)
Ag(110)		0.94 (1.03)	0.51 (0.64)	3.4×10^{3} (2.6×10^{1})	933 (817)	1.63 (1.77)
Ir(111)		0.32 (0.39)	0.09 (0.29)	2.8×10^{8} (5.1×10^{8})	842 (747)	1.48 (1.51)
Pt(111)		0.48 (0.57)	0.40 (0.58)	3.1×10^{6} (3.2×10^{5})	268 (217)	1.68 (1.73)
Cu(111)	CH_3CH_2OH	0.93 (0.91)	-0.02 (0.27)	3.2×10^{2} (1.7×10^{3})	1283 (1190)	1.43 (1.46)

Figure 1. Top (T), Bridge (B), Hexagonal Closed-packed (hcp) Hollow (H), Face-centered Cubic (fcc) Hollow (F), Three-fold Cavity (C_3), Four-fold Cavity (C_4), Top on a Step (T_S), and Bridge on a Step (B_S) Adsorption Sites on the (110), (111) and (211) Miller Index Surfaces of an fcc Metal. Light Grey, Dark Blue, Light Blue, Dark Grey, Pink, and Yellow Spheres Denote Atoms From the First, Second, Third, Fourth, Fifth, and Sixth Atomic Layers in the Direction Perpendicular to the Plane of the Paper, Respectively. The Solid Lines Show the Edges of the Unit Cell and the Dotted Line Marks the Edge of the Step in the (211) Surface.

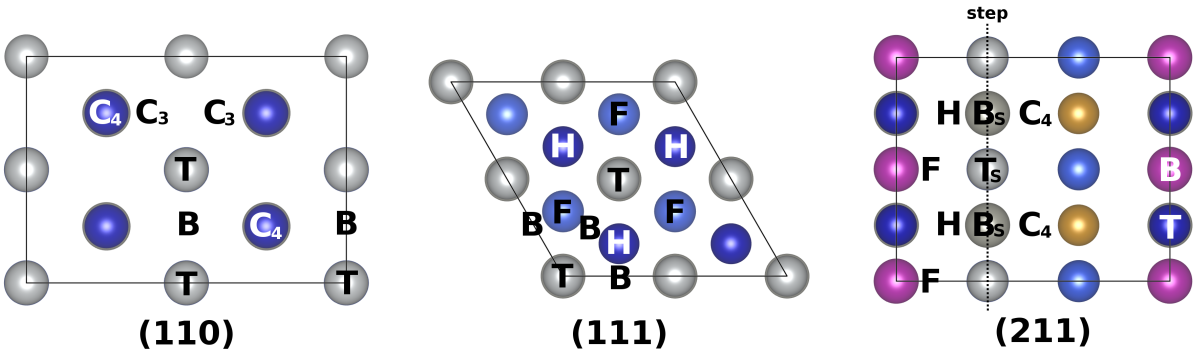

Figure 2. TPSS (Black) and PW91 (Red) Activation Energy Barriers (E^{o}_{act}, eV) Versus Co-adsorption Energies (E^{o}_{coads}, eV) of the Products of the Reaction ROH* + * → RO* + H* (R= CH_3, CH_3CH_2 or H) on Several Metallic Surfaces. W, M, and E Stand for Water, Methanol, and Ethanol Molecules, Respectively.

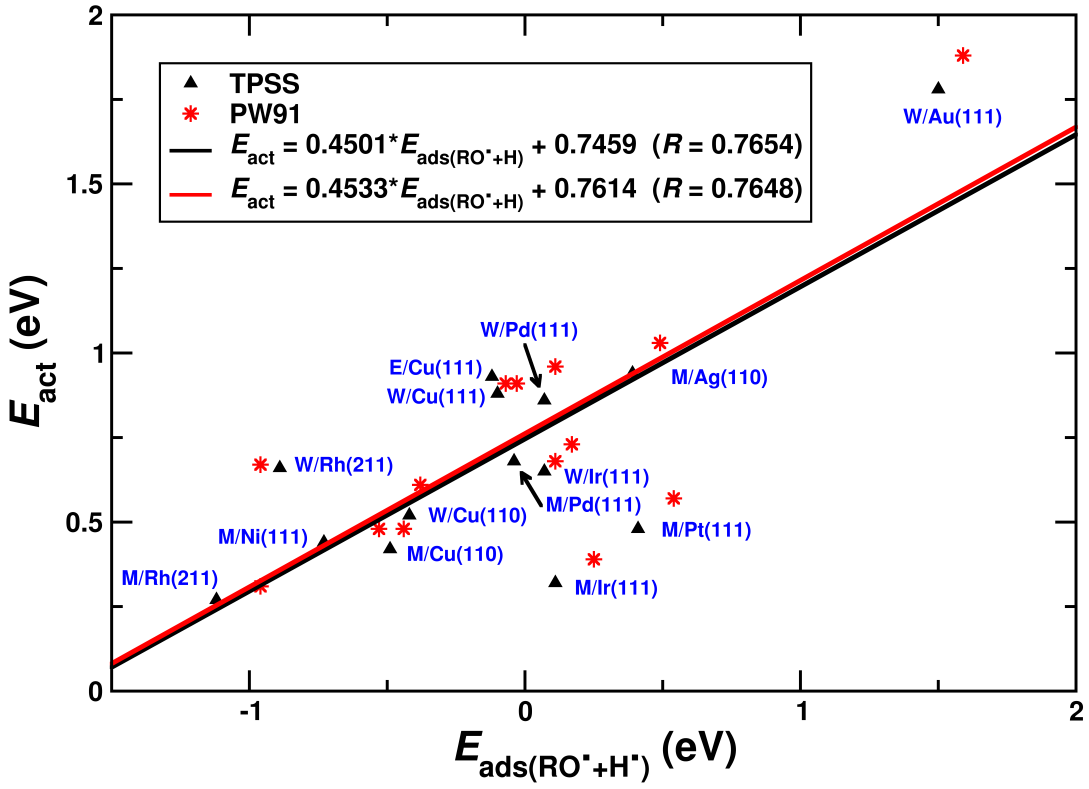

References

(1) J. K. Nørskov, F. Studt, F. Abild-Pedersen and T. Bligaard, *Fundamental Concepts in Heterogeneous Catalysis*, John Wiley & Sons, Inc., **2014**, ISBN: 978-1-118-88895-7.

(2) Van Santen, R. A. Complementary Structure Sensitive and Insensitive Catalytic Relationships. *Acc. Chem. Res.* **2009**, *42*, 57-66.

(3) Van Santen, R. A.; Neurock, M.; Shetty, S. G. Reactivity Theory of Transition-Metal Surfaces: A Brønsted-Evans-Polanyi Linear Activation Energy-Free-Energy Analysis. *Chem. Rev.* **2010**, *110,* 2005–2048.

(4) Fajín, J. L. C.; Cordeiro, M. N. D. S.; Gomes, J. R. B. Water Dissociation on Bimetallic Surfaces: General Trends. *J. Phys. Chem. C* **2012**, *116*, 10120−10128.

(5) Fajín, J. L. C.; Cordeiro, M. N. D. S.; Illas, F.; Gomes, J. R. B. Influence of Step Sites in the Molecular Mechanism of the Water Gas Shift Reaction Catalyzed by Copper. *J. Catal.* **2009**, *268*, 131–141.

(6) Gomes, J. R. B.; Fajín, J. L. C.; Cordeiro, M. N. D. S.; Teixeira, C.; Gomes, P.; Pillai, R. S.; Novell-Leruth, G.; Toda, J.; Jorge, M. Density Functional Treatment of Interactions and Chemical Reactions at Interfaces. In "Density Functional Theory: Principles, Applications and Analysis". Nova Science Publisher, Inc.; Editors: Joseph Morin and Jean Marie Pelletier; New York, second quarter 2013; ISBN: 978-1-62417-955-6.

(7) Brønsted, J. N. Acid and Basic Catalysis. *Chem. Rev.* **1928**, *5*, 231-338.

(8) Evans, M. G.; Polanyi, M. Inertia and Driving Force of Chemical Reactions. *Trans. Faraday Soc.* **1938**, *34*, 11-24.

(9) Pallassana, V.; Neurock, M. Electronic Factors Governing Ethylene Hydrogenation and Dehydrogenation Activity of Pseudomorphic Pd_{ML}/Re(0001), Pd_{ML}/Ru(0001), Pd(111), and Pd_{ML}/Au(111) Surfaces. *J. Catal.* **2000**, *191*, 301-317

(10) Nørskov, J. K.; Bligaard, T.; Logadottir, A.; Bahn, S.; Hansen, L. B.; Bollinger, M.; Bengaard, H.; Hammer, B.; Sljivancanin, Z.; Mavrikakis, M.; Xu, Y.; Dahl, S.; Jacobsen, C. J. H. Universality in Heterogeneous Catalysis. *J. Catal.* **2002**, *209*, 275-278.

(11) Loffreda, D.; Delbecq, F.; Vigné, F.; Sautet, P. Fast Prediction of Selectivity in Heterogeneous Catalysis from Extended Brønsted–Evans–Polanyi Relations: A Theoretical Insight. *Angew. Chem. Int. Ed.* **2009**, *48*, 8978-8980.

(12) Viñes, F.; Vojvodic, A.; Abild-Pedersen, F.; Illas, F. Bronsted-Evans-Polanyi Relationship for Transition Metal Carbide and Transition Metal Oxide Surfaces. *J. Phys. Chem. C* **2013**, *117*, 4168-4171.

(13) Vojvodic, A.; Calle-Vallejo, F.; Guo, W.; Wang, S.; Toftelund, A.; Studt, F.; Martínez, J. I.; Shen, J.; Man, I. C.; Rossmeisl, J.; Bligaard, T.; Nørskov, J. K.; Abild-Pedersen, F. On the Behavior of Brønsted-Evans-Polanyi Relations for Transition Metal Oxides. J. Chem. Phys. **2011**, *134*, 244509.

(14) Fajín, J. L. C.; Cordeiro, M. N. D. S.; Illas, F.; Gomes, J. R. B. Descriptors Controlling the Catalytic Activity of Metallic Surfaces Toward Water Splitting. *J. Catal.* **2010**, *276*, 92-100.

(15) Fajín, J. L. C.; Cordeiro, M. N. D. S.; Gomes, J. R. B. Density Functional Theory Study of the Water Dissociation on Platinum Surfaces: General Trends. *J. Phys. Chem. A* **2014**, *118*, 5832−5840

(16) Fajín, J. L. C.; Bruix, A.; Cordeiro, M. N. D. S.; Gomes, J. R. B.; Illas, F. Density Functional Theory Model Study of Size and Structure Effects on Water Dissociation by Platinum Nanoparticles. *J. Chem. Phys.* **2012**, *137*, 034701-1:10.

(17) Fajín, J. L. C.; Cordeiro, M. N. D. S.; Illas, F.; Gomes, J. R. B. Generalized Brønsted–Evans–Polanyi Relationships and Descriptors for O–H Bond Cleavage of Organic Molecules on Transition Metal Surfaces. *J. Catal.* **2014**, *313*, 24–33.

(18) Perdew, J. P.; Chevary, J. A.; Vosko, S. H.; Jackson, K. A.; Pederson, M. R.; Singh, D. J.; Fiolhais, C. Atoms, Molecules, Solids, and Surfaces: Applications of the Generalized Gradient Approximation for Exchange and Correlation. *Phys. Rev. B* 1992, *46*, 6671-6687.

(19) Perdew, J. P.; Burke, K.; Ernzerhof, M. Generalized Gradient Approximation Made Simple. *Phys. Rev. Lett.* **1996**, *77*, 3865−3868.

(20) Fajín, J. L. C.; Illas, F.; Gomes, J. R. B. Effect of the Exchange-correlation Potential and of Surface Relaxation on the Description of the H_2O Dissociation on Cu(111). *J. Chem. Phys.* **2009,** *130*, 224702-1:8.

(21) Campbell, C. T.; Daube, K. A. A Surface Science Investigation of the Water-gas Shift Reaction on Cu(111). *J. Catal.* **1987**, *104*, 109-199.

(22) Mohsenzadeh, A.; Bolton, K.; Richards, T. DFT Study of the Adsorption and Dissociation of Water on Ni(111), Ni(110) and Ni(100) surfaces, *Surf. Sci.*, **2014**, *627*. 1-10.

(23) Perdew, J. P.; Schmidt, K. Jacob's Ladder of Density Functional Approximations for the Exchange-Correlation Energy. *AIP Conf. Proc*., **2001**, *577*, 1-20.

(24) Yu, H. S.; He, X.; Truhlar, D. G. MN15-L: A New Local Exchange-Correlation Functional for Kohn–Sham Density Functional Theory with Broad Accuracy for Atoms, Molecules, and Solids, *J. Chem. Theory and Comput.*, DOI: 10.1021/acs.jctc.5b01082

(25) Janthon, P.; Kozlov, S. M.; Viñes, F.; Limtrakul, J.; Illas, F. Establishing the Accuracy of Broadly Used Density Functionals in Describing Bulk Properties of Transition Metals. *J. Chem. Theory and Comput.* **2013,** *9*, 1631-1640

(26) Zhao, Y.; Schultz, N. E.; Truhlar, D. G. Design of Density Functionals by Combining the Method of Constraint Satisfaction with Parametrization for Thermochemistry, Thermochemical Kinetics, and Noncovalent Interactions, *J. Chem. Theory and Comput.* **2006,** *2*, 364-382.

(27) Janthon, P.; Luo, S. A.; Kozlov, S. M.; Viñes, F.; Limtrakul, J.; Truhlar, D. G.; Illas, F. Bulk Properties of Transition Metals: A Challenge for the Design of Universal Density Functionals. *J. Chem. Theory Comput*. **2014**, *10*, 3832–3839.

(28) Tao, J. M.; Perdew, J. P.; Staroverov, V. N.; Scuseria, G. E. Climbing the Density Functional Ladder: Nonempirical Meta-Generalized Gradient Approximation Designed for Molecules and Solids. *Phys. Rev. Lett*., **2003**, *91*, 146401-1:4.

(29) Zhao, Y.; Truhlar, D. G. A New Local Density Functional for Main-group Thermochemistry, Transition Metal Bonding, Thermochemical Kinetics, and Noncovalent Interactions. *J. Chem. Phys.* **2006**, *125*, 194101-(1-18).

(30) Peverati, R.; Truhlar, D. G. An Improved and Broadly Accurate Local Approximation to the Exchange–correlation Density Functional: The MN12-L Functional for Electronic Structure Calculations in Chemistry and Physics. *Phys. Chem. Chem. Phys*. **2012**, *14*, 13171-13174.

(31) Janthon, P.; Kozlov, S. M.; Viñes, F.; Limtrakul, J.; Illas, F. Establishing the Accuracy of Broadly Used Density Functionals in Describing Bulk Properties of Transition Metals. *J. Chem. Theory Comput*. **2013**, *9*, 1631-1640.

(32) Staroverov, V. N.; Scuseria, G. E.; Tao, J.; Perdew, J. P. Comparative Assessment of a New Nonempirical Density Functional: Molecules and Hydrogen-bonded Complexes. *J. Chem. Phys*. **2003**, *119*, 12129-12137.

(33) Mardirossian, N.; Parkhill, J. A.; Head-Gordon, M. Benchmark Results for Empirical Post-GGA Functionals: Difficult Exchange Problems and Independent Tests. *Phys. Chem. Chem. Phys.* **2011**, *13*, 19325-19337.

(34) Peverati, R.; Truhlar, D. G. Screened-exchange Density Functionals with Broad Accuracy for Chemistry and Solid-state Physics. *Phys. Chem. Chem. Phys*. **2012**, *14*, 16187-16191.

(35) Peverati, R.; Truhlar, D. G. Quest for a Universal Density Functional: the Accuracy of Density Functionals Across a Broad Spectrum of Databases in Chemistry and Physics. *Philos. Trans. R. Soc*., A **2014**, *372*, 20120476-1:52.

(36) Luo, S.; Zhao, Y.; Truhlar, D. G. Improved CO Adsorption Energies, Site Preferences, and Surface Formation Energies from a Meta-Generalized Gradient Approximation Exchange–Correlation Functional, M06-L. *J. Phys. Chem. Lett*. **2012**, *3*, 2975-2979.

(37) Ferrighi, L.; Madsen, G. K. H.; Hammer, B. Self-consistent Meta-generalized Gradient Approximation Study of Adsorption of Aromatic Molecules on Noble Metal Surfaces. *J. Chem. Phys.* **2011**, *135*, 084704-(1-8).

(38) Toda, J.; Fischer, M.; Jorge, M.; Gomes, J. R. B. Water Adsorption on a Copper Formate Paddlewheel Model of CuBTC: A Comparative MP2 and DFT Study. *Chem. Phys. Lett.* **2013**, *587*, 7-13.

(39) Pueyo Bellafont, N.; Viñes, F.; Illas, F. Performance of the TPSS Functional on Predicting Core Level Binding Energies of Main Group Elements Containing Molecules: A Good Choice for Molecules Adsorbed on Metal Surfaces. *J. Chem. Theory Comput*. **2016**, *12*, 324-331.

(40) Pueyo Bellafont, N.; Álvarez Saiz, G.; Viñes, F.; Illas, F. Performance of Minnesota Functionals on Predicting Core-Level Binding Energies of Molecules Containing Main-Group Elements. *Theor. Chem. Acc*. **2016**, *135*, 35-(1-9).

(41) Broqvist, P.; Alkauskas, A.; Pasquarello, A. Hybrid-functional Calculations with Plane-wave Basis Sets: Effect of Singularity Correction on Total Energies, Energy Eigenvalues, and Defect Energy Levels. *Phys. Rev*. B **2009**, *80*, 085114-(1-13).

(42) Kresse, G.; Hafner, J. Ab Initio Molecular Dynamics for Liquid Metals, *Phys. Rev. B* **1993**, *47*, 558-561.

(43) Kresse, G.; Furthmüller, J. Efficiency of *Ab-initio* Total Energy Calculations for Metals and Semiconductors Using a Plane-wave Basis Set, *Comput*. *Mater*. *Sci*. **1996**, *6*, 15-50.

(44) Kresse, G.; Furthmüller, J. Efficient Iterative Schemes for *Ab-initio* Total Energy Calculations Using a Plane-wave Basis Set. *Phys*. *Rev*. *B* **1996**, *54*, 11169-11186.

(45) Blöchl, P. E. Projector Augmented-wave method, *Phys*. *Rev*. *B* **1994**, *50*, 17953-17979..

(46) Kresse, G.; Joubert, D. From Ultrasoft Pseudopotentials to the Projector Augmented-wave Method, *Phys*. *Rev.B* **1999**, *59*, 1758-1775.

(47) Monkhorst, H. J.; Pack, J. D.Special Points for Brillouin-zone Integrations. *Phys. Rev. B* **1976**, *13*, 5188.

(48) Henkelman, G.; Jónsson, H. A Dimer Method for Finding Saddle Points on High Dimensional Potential Surfaces Using only First Derivatives. *J. Chem. Phys.* **1999**, *111*, 7010-7022.

(49) Laidler, K. J. in: Chemical Kinetics third ed., *Harper Collins*, New York, **1987**, p. 193.

(50) Ayastuy, J. L.; Gutiérrez-Ortiz, M. A.; González-Marcos, J. A.; Aranzabal, A.; González-Velasco, J. R. Kinetics of the Low-Temperature WGS Reaction over a $CuO/ZnO/Al_2O_3$ Catalyst. *Ind. Eng. Chem. Res.* **2005**, *44*, 41-50.

TOC GRAPHICS

Activation energies prediction using BEP relationships